Published OnlineFirst March 29, 2019; DOI: 10.1158/1535-7163.MCT-18-0582

Cancer Biology and Translational Studies

Molecular Cancer Therapeutics

Functional Analysis of Somatic Mutations Affecting Receptor Tyrosine Kinase Family in Metastatic Colorectal Cancer

Leslie Duplaquet[1], Martin Figeac[2], Frédéric Leprêtre[2], Charline Frandemiche[3,4], Céline Villenet[2], Shéhérazade Sebda[2], Nasrin Sarafan-Vasseur[5], Mélanie Bénozène[1], Audrey Vinchent[1], Gautier Goormachtigh[1], Laurence Wicquart[6], Nathalie Rousseau[3], Ludivine Beaussire[5], Stéphanie Truant[7], Pierre Michel[8], Jean-Christophe Sabourin[9], Françoise Galateau-Sallé[10], Marie-Christine Copin[1,6], Gérard Zalcman[11], Yvan De Launoit[1], Véronique Fafeur[1], and David Tulasne[1]

Abstract

Besides the detection of somatic receptor tyrosine kinases (RTK) mutations in tumor samples, the current challenge is to interpret their biological relevance to give patients effective targeted treatment. By high-throughput sequencing of the 58 RTK exons of healthy tissues, colorectal tumors, and hepatic metastases from 30 patients, 38 different somatic mutations in RTKs were identified. The mutations in the kinase domains and present in both tumors and metastases were reconstituted to perform an unbiased functional study. Among eight variants found in seven RTKs (EPHA4-Met726Ile, EPHB2-Val621Ile, ERBB4-Thr731Met, FGFR4-Ala585Thr, VEGFR3-Leu1014Phe, KIT-Pro875Leu, TRKB-Leu584Val, and NTRK2-Lys618Thr), none displayed significantly increased tyrosine kinase activity. Consistently, none of them induced transformation of NIH3T3 fibroblasts. On the contrary, two RTK variants (FGFR4-Ala585Thr and FLT4-Leu1014Phe) caused drastic inhibition of their kinase activity. These findings indicate that these RTK variants are not suitable targets and highlight the importance of functional studies to validate RTK mutations as potential therapeutic targets.

Introduction

Receptor tyrosine kinases (RTK) constitute a large 58-member family in mammals. They all comprise a variable extracellular domain, involved in ligand recognition, and a conserved intracellular tyrosine kinase domain. RTKs regulate a broad spectrum of biological responses, including differentiation, proliferation, motility, and survival. They are also all involved, through ligand/receptor interactions, in the dialogue between tissues of pluricellular organisms. Binding of the ligand to the extracellular domain of an RTK favors its dimerization and modifies its conformation, causing activation of its intracellular tyrosine kinase domain. Subsequent tyrosine phosphorylation in the intracellular domain of the RTK allows recruitment of signaling proteins responsible for signal propagation (1).

RTKs are often found deregulated in cancer, as a result of various molecular alterations leading to their activation. These alterations include mutations, translocations, and gene amplifications. Single nucleotide variants with missense mutations are frequently found in cancer, and are directly responsible of RTK activation. Most RTK-activating mutations have been found in the kinase domain. Examples include the EGFR L858R missense mutation in non–small cell lung cancers (NSCLC; ref. 2), KIT D816V in mastocytosis (3), FLT3 D835N in acute myeloid leukemia (AML ref. 4), and ALK F1174L in neuroblastoma (5). RTKs have also been found mutated in regions other than the tyrosine kinase domain, including the extracellular ligand-binding domain, but the functional consequences of these mutations are often uncharacterized.

RTK mutation rates in cancer vary according to the cancer type and the RTK. For instance, the D816V variant of KIT was found in 90% of systemic mastocytosis cases (6). Most of the time, however, RTK mutations represent less than 10% of the molecular alterations found in a given cancer type. For instance, EGFR mutations account for 10% to 12% of the molecular alterations found in NSCLC (7) and FLT3 mutations represent about 7% of those found in AML (4). In addition, many different activating

[1]Univ. Lille, CNRS, Institut Pasteur de Lille, UMR 8161 - M3T, Lille, France. [2]Univ. Lille, Plateau de génomique fonctionnelle et structurale, CHU Lille, Lille, France. [3]TCBN - Tumorothèque Caen Basse-Normandie, Caen, France. [4]Réseau Régional de Cancérologie, OncoBasseNormandie, Caen, France. [5]Normandie Univ, UNIROUEN, Inserm U1245, IRON group, Rouen University Hospital, Normandy Centre for Genomic and Personalized Medicine, Rouen, France. [6]Tumorothèque du C2RC de Lille, Lille, France. [7]Department of Digestive Surgery and Transplantation, CHU Lille, Univ Lille, Lille Cedex, France. [8]Department of Hepato-Gastroenterology, Rouen University Hospital, Normandie Univ, UNIROUEN, Inserm U1245, IRON group, Rouen, France. [9]Department of Pathology, Normandy University, INSERM 1245, Rouen University Hospital, Rouen, France. [10]Department of Pathology, MESOPATH-MESOBANK, Centre Léon Bérard, Lyon, France. [11]Thoracic Oncology Department, CIC1425/CLIP2 Paris-Nord, Hôpital Bichat-Claude Bernard, Paris, France.

Note: Supplementary data for this article are available at Molecular Cancer Therapeutics Online (http://mct.aacrjournals.org/).

Corresponding Author: David Tulasne, French National Centre for Scientific Research, 1 Rue Pr Calmette, Lille, 59021, France. Phone: 333-2087-1257; Fax: 333-2087-1111; E-mail: david.tulasne@ibl.cnrs.fr

Mol Cancer Ther 2019;18:1137–48

doi: 10.1158/1535-7163.MCT-18-0582

Published OnlineFirst March 29, 2019; DOI: 10.1158/1535-7163.MCT-18-0582

mutations are liable to affect a given RTK. In papillary renal cell carcinomas, for instance, seven different MET-activating mutations have been characterized (8).

Recent advances in high-throughput sequencing of genomic DNA and mRNA have revealed the considerable diversity of RTK mutations in cancer, as recorded in the COSMIC database (https://cancer.sanger.ac.uk/cosmic). For instance, genomic sequencing data extracted from several studies and compiled in the COSMIC database reveal more than a thousand ERBB4 mutations among 39,846 tumor samples. Only some of these have been functionally studied, but this has notably revealed the existence of two ERBB4-activating mutations in NSCLC of which clinical impact is still unknown (9). In most other RTKs, likewise, many mutations have been described, but the functional consequences of most of them, including missense mutations in the kinase domain, have not yet been investigated. Thus, because activating mutations in RTKs are diverse and often present at low rates in cancer, it is hard to know whether an RTK alteration revealed by high-throughput sequencing can lead to receptor activation.

Despite these difficulties, characterizing RTK alterations is clinically crucial, because many recent targeted therapies, under development or already used clinically, are directed against members of this receptor family. This applies notably to melanoma, leukemia, and lung, breast, and colorectal cancers (10–12). The inhibitors used in such therapies include mAbs that prevent ligand/receptor binding or receptor dimerization and tyrosine kinase inhibitors (TKI) inhibiting tyrosine kinase activity. Importantly, the efficacy of these targeted therapies depends on the presence, in the targeted RTK, of molecular alterations leading (i) to its unambiguous activation (ii) to a dependency for cell survival on this mutation, the so-called "oncogene addiction", both characteristics defining a driver mutation (for a review see ref. 13). For example, TKIs targeting EGFR can be used to treat patients with NSCLC whose tumors harbor EGFR-activating mutations (14).

Colorectal cancer is the third most common cancer worldwide, with about 1.4 million cases in 2012 (15). The early stage is highly curable, mainly by surgery, radiotherapy, and adjuvant chemotherapy. About half of all patients with colorectal cancer, however, display metastases either at diagnosis (synchronic metastases) or after resection of the primary tumor. These metastases are mainly located in the liver (16). Importantly, the 5-year survival of metastatic colorectal cancer patients is only about 10% (French National Cancer Institute, 2010 Report). Although liver metastases can be resected surgically, the treatment of metastatic disease is based mainly on chemotherapy and, more rarely, on targeted therapies (17).

Many well-known genomic alterations have been identified in colorectal cancer, including KRAS- and PI3K-activating mutations found, respectively, in about 40% and 15% of colorectal cancers. Tumor suppressor–inactivating mutations are also often found in colorectal cancer, such as mutations in APC or p53 (18). All these alterations are frequently found in both tumor and metastatic samples, which confirms their importance in tumor progression (19). None of these alterations, however, is targetable by current novel targeted therapies (17).

Interestingly, some RTK alterations have recently been characterized in advanced colorectal cancer. According to The Cancer Genome Atlas consortium, for instance, HER2 gene amplification or HER2 somatic mutations are present in 7% of patients with colorectal cancer (20). Mutations in the HER kinase domain, already identified as activating mutations in breast cancer, have been shown to induce HER2 activation and transformation of colorectal cell lines (21). Translocation of the *TRKA* gene, leading to constitutive activation of its kinase domain and likewise resulting in cell transformation, has also been found in colorectal cancer, albeit in less than 2% of cases (22). Finally, treatment with mAbs directed against EGFR has proven effective, provided that KRAS was not mutated (23). The efficacy of this treatment could be related to ligand-dependent activation of EGFR via an autocrine activation loop (24). Altogether, these recent findings reveal that RTK alterations, including somatic mutations, occur at a relatively low rate in colorectal cancer. They might open the way for treatments specifically targeting RTK variants.

The above findings have led us to wonder whether other targetable RTK mutations might be present in colorectal cancer. To answer this question, we performed deep high-throughput sequencing of the 58 RTK and control genes frequently mutated in colorectal cancer. We chose to sequence healthy tissues, tumors, and hepatic metastases from each of 30 patients, firstly to eliminate constitutional mutations present in healthy tissues and secondly to select mutations present in both tumors and metastases, like the currently well-known driver mutants. Identified RTK mutations located in the kinase domain and present in both tumors and metastases were further analyzed functionally, in a systematic fashion, to evaluate their ability or inability to activate the kinase.

Materials and Methods

Sample preparation and DNA extraction

The samples were used in accordance to the legislation of two French biobanks, "Tumorothèque Caen Basse-Normandie (TCBN)" and "Tumorothèque C2RC de Lille," which are certified in conformity with the norm AFNOR NF-S 96-900 (Quality of Biological Resources Centers) and in accordance to the International Ethical Guidelines for Biomedical Research Involving Human Subjects. Investigators obtained informed written consent from the patients.

All tissue samples were collected from 30 patients who underwent surgical resection for metastatic colorectal cancer between 2004 and 2012. For each patient, colorectal tumor tissue, colorectal nontumoral tissue, and hepatic metastasis tissue were selected. At the time of resection, the specimens were transported in identified containers at 4°C or room temperature. The transport time was generally <30 minutes. The specimens were examined by a pathologist and were oriented, measured, and described. Tumor bank's tissues were collected in a range that did not affect diagnosis. After removal, tumor tissues of $0.5 \times 0.5 \times 0.5$ cm^3 were stored in labeled cryovials and snap-frozen in liquid nitrogen, and then transferred and stored at −80°C until DNA extraction. Clinical data for these samples are shown in Table 1.

For the DNA extraction, commercial DNA extraction kits (Qiagen, QIAamp DNA Mini QIAcube Kit) were used as per manufacturer's instructions. A total of 60 to 80 20-µm-thick sections were cut with a cryostat and were homogenized in the supplied lysis buffer with Proteinase K. All samples were incubated at 56°C for 1 night under agitation (1,100 rpm). The DNA was bound to a spin column filter, then washed with 96%–100% ethanol, followed by two wash buffers (supplied). The bound DNA was eluted from the spin column filter with the supplied elution buffer. Absorbance measurements were made on a spectrophotometer (Nanovue).

Published OnlineFirst March 29, 2019; DOI: 10.1158/1535-7163.MCT-18-0582

Table 1. Clinical data pertaining to the 30 patients with metastatic colorectal cancer

	Chemo-naïve group	Chemo-treated group	Overall
Total number of patients	8	22	30
Age onset colorectal cancer diagnosis, y (a)			
Mean	71, 37	59, 54	65, 45
Range	57–78	36–78	36–78
Gender			
Males; females	5; 3	13; 9	18; 12
Tumor localization			
Right colon	7	7	14
Left colon	0	3	3
Transverse colon	0	1	1
Sigmoid	1	8	9
Rectum	0	3	3
Time between primary tumor resection and metastasectomy, mo			
Mean	3, 4	6, 24	4, 82
Range	0–34	0–26	0–34
Overall survival time, y			
Mean	3.9 ± 1.1	5.2 ± 0.4	5.0 ± 0.4
No. of patients who died from disease	3	9	12
Chemotherapeutic schedule (b)			
Folfiri	–	2	2
Folfiri + Avastin	–	5	5
Folfox	–	9	9
Folfox + Avastin	–	2	2
Xelox	–	1	1
Erbitux + Xelox (Xeloda-Oxaliplatine)	–	1	1
Folfox + LV5 FU2	–	1	1
Xeloda + 5FU/Leucoverine	–	1	1
pTNM Classification			
T3	4	16	20
T4	3	3	6
T4b	1	–	1
Nx	1	–	1
N0	3	10	13
N1	5	4	9
N1a	1	–	1
N1b	1	–	1
N2	–	2	2
N2a	1	–	1
N2b	1	–	1
Mx	1	5	6
M1	6	15	21
M1b	–	1	1
M2	–	–	–

NOTE: Some patients had received chemotherapy (chemo-treated) and others, not (chemo-naïve). For the former patients, the chemotherapy administered and treatment schedule are detailed. Patient gender and age at diagnosis are indicated. Primary tumor location and the time in months between tumor and metastasis resection are detailed, as is the pTNM classification. Overall survival in years is presented.

Finally, the DNA samples were sent to the Functional and Structural Genomic Platform (Lille, France).

Targeted next-generation sequencing

A haloplex panel was designed to cover the 58 RTK genes plus the KRAS and PI3KCA oncogenes and the TP53 tumor suppressor gene. The panel was designed for Illumina sequencers on Agilent's SureDesign website (https://earray.chem.agilent.com/suredesign/index.htm). It covers whole exonic coding sequences with a 10-base offset in intronic sequences of our targeted genes and consists of 17,116 amplicons covering 230,179 bases of the human genome (hg19, GRCh37 assembly). The panel was manufactured by Agilent and is available on request.

Library preparation and sequencing

Libraries were prepared with the HaloPlex Target Enrichment Kit (Agilent) according to the manufacturer's instructions except that we used 125-ng starting DNA instead of 250 ng. Briefly, samples were digested with eight different restriction enzymes and enriched in the target regions by using highly specific biotinylated complementary probes. Hybridized probes were captured with magnetic beads and target fragments were ligated to create circular DNA molecules. After the libraries were amplified by PCR, they were pooled in equimolar amounts in two pools. Sequencing was performed on two lanes of a Hi-Seq Illumina sequencer (Illumina, Inc.). Sequencing data were deposited to Sequence Read Archive with the accession number PRJNA528252.

Cytokines, drugs, and cell cultures

SCF and BDNF were purchased from Peprotech, and imatinib and entrectinib (25) were purchased from Selleckchem. HEK293 cells were cultured in DMEM (Invitrogen) supplemented with 10% heat-inactivated FCS (Invitrogen) and antibiotics. NIH3T3 cells were cultured in DMEM supplemented with 10% bovine calf

Published OnlineFirst March 29, 2019; DOI: 10.1158/1535-7163.MCT-18-0582

serum (Invitrogen) and antibiotics. HCT-116 cells were cultured in McCoy's 5A medium (Invitrogen) supplemented with 10% FCS and antibiotics.

Western blot analyses

Western blotting was performed as described previously (26). Samples were resolved by 10% SDS-polyacrylamide gel electrophoresis or precast 4% to 12% Gradient Gel (Thermo Fisher Scientific). For quantification of protein expression, luminescence was captured with a digital imaging using a cooled Charge Coupled Device Camera (LAS 3000), and quantification was performed using Multigauge V3.0 software. The background-adjusted volume was normalized to empty well.

Transfection and NIH3T3 transformation

NIH3T3 cells (300,000 cells in a 6-well plate) were transfected with FuGENE HD (Promega; 2 μg DNA/8 μL FuGENE in 100 μL Opti-MEM medium, Thermo Fisher Scientific). The next day, the cells were transferred to a 100-mm plate and cultured 2 days later in 5% calf serum medium. Fifteen days later, the cells were fixed in fast green/methanol and stained with Carazzi/Eosin.

Sanger sequencing

Primers for next-generation sequencing (NGS) variant validation were designed with the Oligo7 software. Primer sequences are described in Supplementary Figure S2. Patient sample DNA was amplified by PCR, sequenced by Sanger sequencing, and analyzed with Chromas software.

Mutagenesis

Substitution mutagenesis was performed with the QuikChange II XL Kit (Stratagene) according to an adapted protocol (27). Plasmids and primers are described in Supplementary Fig. S3. The two complementary primers used for mutagenesis were designed to contain appropriate base changes. Briefly, a two-step PCR was performed to insert mutations into plasmids. A first, three-cycle PCR was completed with a single primer (forward or reverse) to promote elongated primer hybridization. The PCR products were then mixed and a second, 18-cycle conventional PCR was carried out. The generated PCR products were treated with Dpn1 enzyme to digest the parental plasmids. Total DNA was purified by phenol-chloroform extraction and then precipitated with isopropanol to improve transformation of TAM1-competent *Escherichia coli*. Successful introduction of mutations was checked by Sanger sequencing.

RTK 3D kinase structure

Three-dimensional (3D) structures of the RTK kinase domains were downloaded from the Protein Data Bank (PDB; www.rcsb.org) with the following PDB IDs: 4asz for NTRK2, 4qqt for FGFR4, 4u0i for KIT, 2r2p for EphA5, 2y6m for EphA4, 3zfm EphB2, 3bbw for ERBB4, and 3hng for VEGFR1. The mutated amino acids of the kinase domain were modified with Swiss-pdb Viewer 4.1.0 software and final pictures were produced with NGL viewer 0.10.4 software.

Results

Targeted NGS of genomic DNA from healthy tissues, colorectal tumors, and hepatic metastases

Thirty patients with colorectal cancer and hepatic metastases, with available frozen surgical samples of healthy, tumor, and metastatic tissues, were identified in three hospitals located in the north of France. Twenty-two patients had received chemotherapy before the surgery and 8 were naïve of treatment. The clinical data concerning these patients are summarized in Table 1. Centralized anatomopathologic analysis confirmed the normal or pathologic status of each sample. All the selected patients displayed at least 50% pathologic tissue in the tumor and metastasis samples and 100% normal tissue in the healthy tissue sample.

Genomic DNA was extracted from each sample and targeted NGS was performed to sequence all the exons of the 58 RTK genes and of three genes frequently mutated in metastatic colorectal cancers use as internal control for sequencing robustness: the KRAS and PI3KCA oncogenes and the tumor suppressor gene, TP53.

Alignment of the raw data with the hg19 genome was performed with Novalign software and produced a total of 20,538,106,880 bases, with a mean depth of 2158 bases per sample. Variant calling performed with FreeBayes software produced 871 individual variants, which were annotated with Annovar software. The list of variants was reduced to 325 variants after filtering out the variants found in normal tissues to exclude nonsomatic ones. After exclusion of variants found in databases, this list was limited to 321 variants, and after selection according to their positions with respect to CDS sequences and splicing sites, followed by elimination of synonymous variants, there remained 233 variants. Finally, we filtered this last list according to the variant-calling quality (at least 40 in QUAL) and produced 68 candidate variants for functional analysis (Fig. 1).

In tumors and metastatic tissues, RTKs displayed 38 different, mainly unknown, somatic mutations

After the selection process, the 68 remaining variants included 38 different mutations in RTKs and 30 different mutations in KRAS, PI3KCA, or TP53 (Fig. 2; Supplementary Table S1 for details of all variants). In this pool of variants some, such as KRAS G12V, were found several times, in different patients. In all, the 30 patients displayed 50 mutations in KRAS, PI3KCA, or TP53. All of these had previously been included in somatic mutation databases (Supplementary Table S1) and 78% (39/50) of them were found in both the tumor and the metastatic tissue of the patient concerned (Fig. 2), as described previously for some of these well-known driver mutations (19).

All the KRAS mutations described at time of clinical diagnosis, mainly by SNaPshot, were subsequently confirmed by NGS (10/10). Other patients, not tested at diagnosis, also displayed KRAS mutations in our sequencing process. This brought to 60% (18/30) the proportion of patients with KRAS mutations (Supplementary Fig. S1). Confirmation of the KRAS mutations found at diagnosis and the fact that all the KRAS, PI3KCA, and TP53 variants had already been described validated the quality of sequencing and the variant selection process.

In RTK genes, 38 different somatic mutations were identified in 20 patients. Ten patients did not harbor any RTK somatic mutation. Each mutation was found only once among the 20 patients. Half of these variants were not reported in the examined main variant data bases (Supplementary Table S1). We found 44% of the mutations (17/38) in both the tumor and the metastatic tissue from the patient concerned. The others were about equally distributed between the tumor (9 variants) and the metastatic tissue (12 variants). Among the 58 RTKs, less than half harbored somatic mutations (24 RTK) and some of them, such as EPHA4, EPHA5,

Published OnlineFirst March 29, 2019; DOI: 10.1158/1535-7163.MCT-18-0582

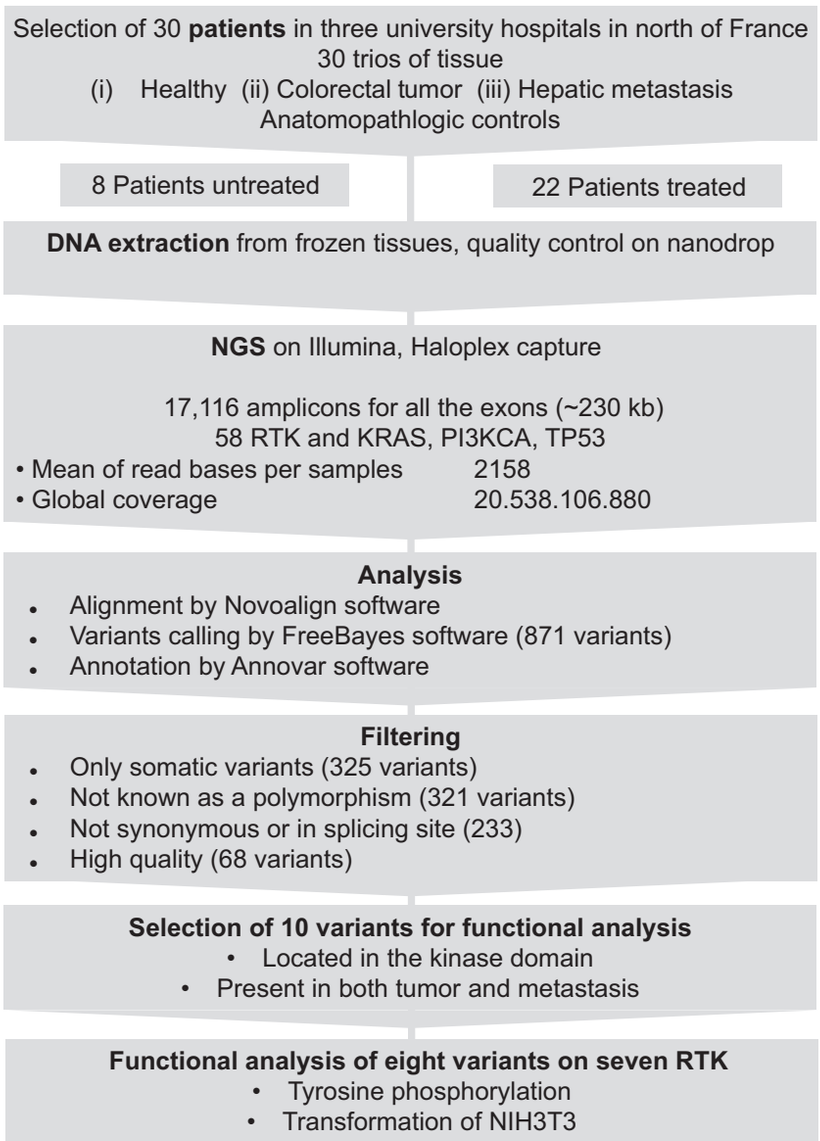

Figure 1.
Flow chart of the experimental procedure. Diagram of the main experimental steps of the study, including (i) selection of 30 patients with metastatic colorectal cancer at the university hospitals of Caen, Lille, and Rouen in the north of France; (ii) extraction and quality control of DNA from frozen healthy, tumor, and metastatic tissues; (iii) NGS sequencing of all RTK exons and, as controls, KRAS, PI3KCA, and TP53; (iv) bioinformatic analysis to identify somatic mutations in RTKs; (v) selection of somatic variants; and (vi) functional analysis, including assessment of RTK tyrosine phosphorylation and transforming potential.

ERBB4, FGFR4, NTRK2, or FLT4, harbored several different mutations (Supplementary Fig. S1). Interestingly, 50% (19/38) of the variants were located in the tyrosine kinase domain of the RTK (Fig. 2; Supplementary Table S1).

Subselection and validation of variants for further functional analysis

Next, we subselected a reasonable number of variants suitable for performing further functional analyses aiming to evaluate their impact on RTK activity. First, we selected mutations present in both the tumor and the metastatic tissue, that is, 17 variants of the 38. This choice was made because most of the known driver mutations affecting KRAS, PI3KCA, or TP53 have been found in both types of tumor tissues. Then, among these 17 variants, we selected the somatic mutations affecting the kinase domain of the RTK, that is, 10 mutations, as most RTK-activating somatic mutations are located in the kinase domain. Representative examples include EGFR mutations in lung cancer (14) and MET mutations in papillary renal cell carcinoma (8).

The 10 mutations affecting the 9 RTK genes are the following: EPHA2-Val800Met, EPHA4-Met726Ile, EPHA5-Arg694Cys, EPHB2-Val621Ile, ERBB4-Thr731Met, FGFR4-Ala585Thr, VEGFR3-Leu1014Phe(FLT4), KIT-Pro875Leu, TRKB-Leu584Val(NTRK2), and TRKB-Lys618Thr (highlighted in Fig. 2). Before functional analysis, Sanger sequencing of these mutations was performed, after amplification by PCR, on genomic DNA from the healthy, tumor, and metastatic tissues (Supplementary Fig. S2). All but one of the variants were absent from the normal tissue but present in both the tumor and metastatic tissue. The exception was EPHB2-Val621Ile, present in the metastatic tissue but not in the tumor sample. The allelic ratio found by NGS (0.1) was below the detection limit of Sanger sequencing (Supplementary Fig. S2). Thus, Sanger sequencing confirmed the NGS data and validated the choice of the selected variants.

Published OnlineFirst March 29, 2019; DOI: 10.1158/1535-7163.MCT-18-0582

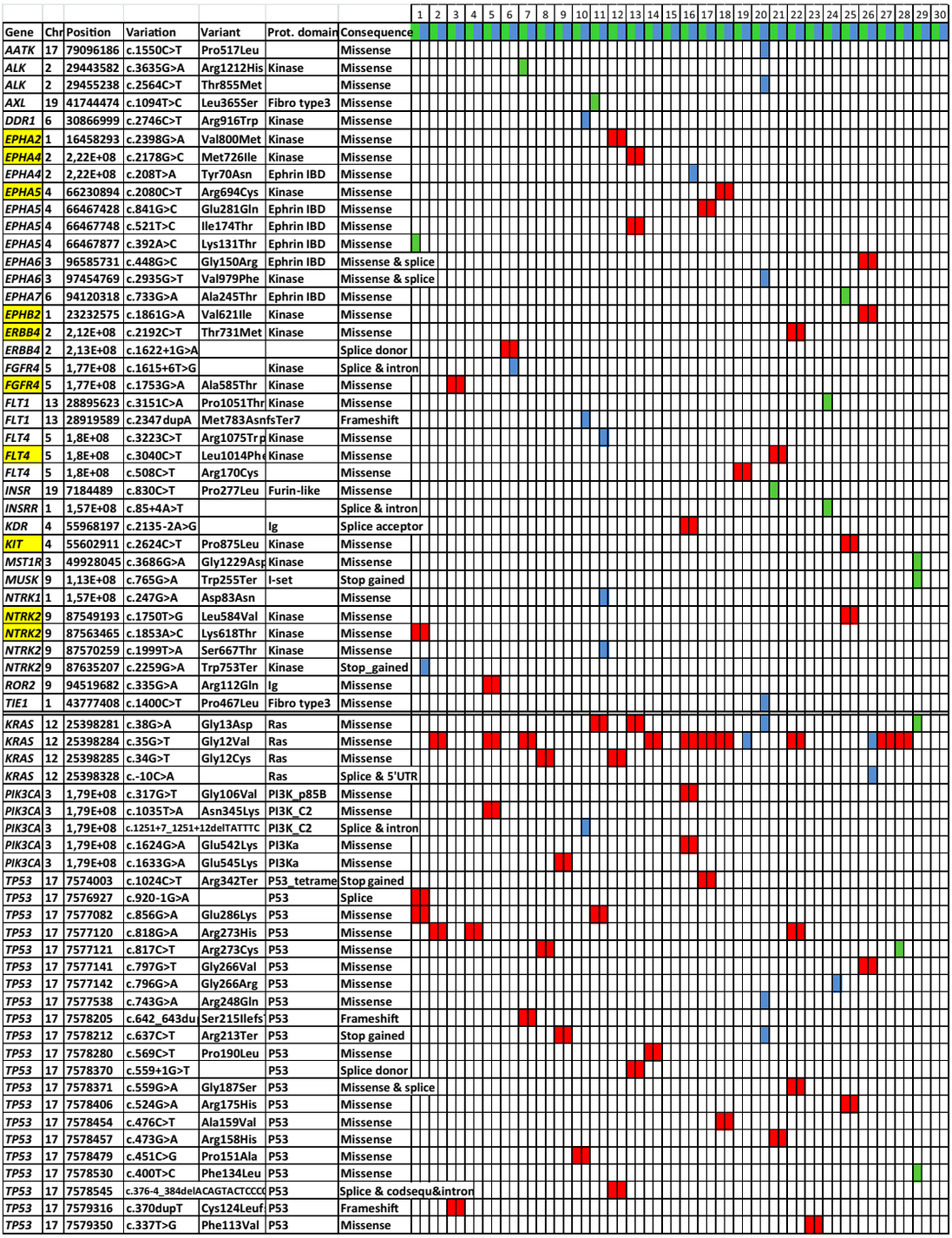

Gene	Chr	Position	Variation	Variant	Prot. domain	Consequence
AATK	17	79096186	c.1550C>T	Pro517Leu		Missense
ALK	2	29443582	c.3635G>A	Arg1212His	Kinase	Missense
ALK	2	29455238	c.2564C>T	Thr855Met		Missense
AXL	19	41744474	c.1094T>C	Leu365Ser	Fibro type3	Missense
DDR1	6	30866999	c.2746C>T	Arg916Trp	Kinase	Missense
EPHA2	1	16458293	c.2398G>A	Val800Met	Kinase	Missense
EPHA4	2	2,22E+08	c.2178G>C	Met726Ile	Kinase	Missense
EPHA4	2	2,22E+08	c.208T>A	Tyr70Asn	Ephrin IBD	Missense
EPHA5	4	66230894	c.2080C>T	Arg694Cys	Kinase	Missense
EPHA5	4	66467428	c.841G>C	Glu281Gln	Ephrin IBD	Missense
EPHA5	4	66467748	c.521T>C	Ile174Thr	Ephrin IBD	Missense
EPHA5	4	66467877	c.392A>C	Lys131Thr	Ephrin IBD	Missense
EPHA6	3	96585731	c.448G>C	Gly150Arg	Ephrin IBD	Missense & splice
EPHA6	3	97454769	c.2935G>T	Val979Phe	Kinase	Missense & splice
EPHA7	6	94120318	c.733G>A	Ala245Thr	Ephrin IBD	Missense
EPHB2	1	23232575	c.1861G>A	Val621Ile	Kinase	Missense
ERBB4	2	2,12E+08	c.2192C>T	Thr731Met	Kinase	Missense
ERBB4	2	2,13E+08	c.1622+1G>A			Splice donor
FGFR4	5	1,77E+08	c.1615+6T>G		Kinase	Splice & intron
FGFR4	5	1,77E+08	c.1753G>A	Ala585Thr	Kinase	Missense
FLT1	13	28895623	c.3151C>A	Pro1051Thr	Kinase	Missense
FLT1	13	28919589	c.2347dupA	Met783AsnfsTer7		Frameshift
FLT4	5	1,8E+08	c.3223C>T	Arg1075Trp	Kinase	Missense
FLT4	5	1,8E+08	c.3040C>T	Leu1014Phe	Kinase	Missense
FLT4	5	1,8E+08	c.508C>T	Arg170Cys		Missense
INSR	19	7184489	c.830C>T	Pro277Leu	Furin-like	Missense
INSRR	1	1,57E+08	c.85+4A>T			Splice & intron
KDR	4	55968197	c.2135-2A>G		Ig	Splice acceptor
KIT	4	55602911	c.2624C>T	Pro875Leu	Kinase	Missense
MST1R	3	49928045	c.3686G>A	Gly1229Asp	Kinase	Missense
MUSK	9	1,13E+08	c.765G>A	Trp255Ter	I-set	Stop gained
NTRK1	1	1,57E+08	c.247G>A	Asp83Asn		Missense
NTRK2	9	87549193	c.1750T>G	Leu584Val	Kinase	Missense
NTRK2	9	87563465	c.1853A>C	Lys618Thr	Kinase	Missense
NTRK2	9	87570259	c.1999T>A	Ser667Thr	Kinase	Missense
NTRK2	9	87635207	c.2259G>A	Trp753Ter	Kinase	Stop_gained
ROR2	9	94519682	c.335G>A	Arg112Gln	Ig	Missense
TIE1	1	43777408	c.1400C>T	Pro467Leu	Fibro type3	Missense
KRAS	12	25398281	c.38G>A	Gly13Asp	Ras	Missense
KRAS	12	25398284	c.35G>T	Gly12Val	Ras	Missense
KRAS	12	25398285	c.34G>T	Gly12Cys	Ras	Missense
KRAS	12	25398328	c.-10C>A		Ras	Splice & 5'UTR
PIK3CA	3	1,79E+08	c.317G>T	Gly106Val	PI3K_p85B	Missense
PIK3CA	3	1,79E+08	c.1035T>A	Asn345Lys	PI3K_C2	Missense
PIK3CA	3	1,79E+08	c.1251+7_1251+12delTATTTC		PI3K_C2	Splice & intron
PIK3CA	3	1,79E+08	c.1624G>A	Glu542Lys	PI3Ka	Missense
PIK3CA	3	1,79E+08	c.1633G>A	Glu545Lys	PI3Ka	Missense
TP53	17	7574003	c.1024C>T	Arg342Ter	P53_tetrame	Stop gained
TP53	17	7576927	c.920-1G>A		P53	Splice
TP53	17	7577082	c.856G>A	Glu286Lys	P53	Missense
TP53	17	7577120	c.818G>A	Arg273His	P53	Missense
TP53	17	7577121	c.817C>T	Arg273Cys	P53	Missense
TP53	17	7577141	c.797G>T	Gly266Val	P53	Missense
TP53	17	7577142	c.796G>A	Gly266Arg	P53	Missense
TP53	17	7577538	c.743G>A	Arg248Gln	P53	Missense
TP53	17	7578205	c.642_643du	Ser215Ilefs	P53	Frameshift
TP53	17	7578212	c.637C>T	Arg213Ter	P53	Stop gained
TP53	17	7578280	c.569C>T	Pro190Leu	P53	Missense
TP53	17	7578370	c.559+1G>T		P53	Splice donor
TP53	17	7578371	c.559G>A	Gly187Ser	P53	Missense & splice
TP53	17	7578406	c.524G>A	Arg175His	P53	Missense
TP53	17	7578454	c.476C>T	Ala159Val	P53	Missense
TP53	17	7578457	c.473G>A	Arg158His	P53	Missense
TP53	17	7578479	c.451C>G	Pro151Ala	P53	Missense
TP53	17	7578530	c.400T>C	Phe134Leu	P53	Missense
TP53	17	7578545	c.376-4_384delA	CAGTACTCCC	P53	Splice & codsequ&intron
TP53	17	7579316	c.370dupT	Cys124Leuf	P53	Frameshift
TP53	17	7579350	c.337T>G	Phe113Val	P53	Missense

Figure 2.

Somatic mutations in the 58 RTKs, KRAS, PI3KCA, and TP53 in tumors and metastases of the 30 patients. Presentation of the 38 somatic mutations in RTKs and 30 somatic mutations in KRAS, PI3KCA, or TP53 absent from normal tissues but present in the colorectal tumors (green column) and/or hepatic metastases (blue column) of the 30 patients. For each variant (columns on the left), the genomic position (position), chromosome (Chr), and gene name (Gene) are supplied, The AA substitution (variant), functional domain affected (protein domain), and type of mutation (consequence; missense, splice donor/acceptor, frameshift, stop gained) are indicated. Variants are labeled, respectively, in green, blue, or red according to their presence in the tumor, the metastatic tissue, or both.

Published OnlineFirst March 29, 2019; DOI: 10.1158/1535-7163.MCT-18-0582

The somatic mutations either inhibit kinase activity or do not modify it

For functional analysis, the somatic mutations were reconstituted by directed mutagenesis in expression vectors for the relevant RTKs (Supplementary Fig. S3). For EPHA2 and EPHA5, no expression vector was found in any academic laboratory. We were thus able to reconstitute eight somatic mutations in seven different RTKs. All constructs were verified by Sanger sequencing. The receptors were detected with commercially available antibodies specifically recognizing the receptor itself (TRKB/NTRK2, VEGFR3/FLT4, KIT) or a fused C-terminal *tag* (FGFR4-*HA*, ERBB4-*HA*, EPHB2-*MYC*, EPHB4-*FLAG*). The tyrosine-phosphorylated form of each RTK was detected with commercially available antibodies directed against one or more intracellular phosphorylated tyrosine residue(s) specific to that RTK. The antibodies used are listed in Supplementary Fig. S3.

HEK-293T cells were transfected with rising concentrations of a vector expressing either a wild-type (WT) or a mutated version of the RTK to be studied, and RTK expression and phosphorylation were evaluated by Western blotting. The ERBB4 receptor could not be functionally analyzed because transfection did not lead to a detectable level of receptor. In all other cases, transfection with increasing amounts of vector led to increasing levels of WT or mutated receptor (Figs. 3 and 4). For FGFR4, maximal expression of the receptor gene was observed already at the smallest DNA concentration tested (0.25 μg), suggesting that expression from this vector is highly efficient in HEK293 cells (Fig. 4A). For VEGFR3 (FLT4) and TRKB (NTRK2), the amount of receptor produced appeared first to rise as the amount of transfecting DNA increased, but then to drop as it increased further, suggesting either a decrease of the transfection efficiency at high DNA concentration or cell toxicity of the receptor produced (Figs. 3I and 4C). In all cases, the levels of the WT and mutated RTK were generally similar along the dose–response curve, demonstrating that the mutations do not affect receptor expression or stability. Reprobing with antibodies directed specifically against tyrosine-phosphorylated forms showed that all the WT RTKs were phosphorylated in cells transiently transfected without ligand stimulation. Ligand-independent phosphorylation upon transient transfection has previously been observed for other RTKs (28), a likely consequence of overexpression. The mutated forms EPHA4-Met726Ile, EPHB2-Val621Ile, KIT-Pro875Leu, TRKB-Leu584Val (*NTRK2* gene), and TRKB-Lys618Thr displayed phosphorylation levels similar to those of their respective WT forms (Fig. 3A, C, E, G, and I). In contrast, the mutated forms, FGFR4-Ala585Thr and VEGFR3-Leu1014Phe (*FLT4 gene*), displayed no detectable tyrosine phosphorylation whatever the vector concentration used (Fig. 4A and C). Similar absence of detectable VEGFR3-Leu1014Phe phosphorylation was obtained in human colorectal carcinoma cells HCT-116 (Fig. 4E). Western blotting quantifications for two representative situations confirmed abolition of tyrosine phosphorylation of the FGFR4 Ala585Thr variant and absence of effect for TRKB Lys618Thr and Leu584Ile variants (Supplementary Fig. S4). Response to ligand stimulation was also investigated for KIT and TRKB receptors. Nor the KIT ligand, SCF, or the TRKB ligand, BDNF, increased tyrosine phosphorylation of their respective WT or mutated receptor (Supplementary Fig. S5). Nevertheless, it is worth noticing that transient transfection induced their constitutive phosphorylation that can mask ligand stimulation. Furthermore, phosphorylation inhibition by TKI, used for patient treatment, was tested for WT and mutated forms of KIT and TRKB. The KIT inhibitor, imatinib, and TRKB inhibitor, entrectinib, were able to inhibit phosphorylation of WT and mutated KIT and TRKB stimulated or not by their respective ligand, indicating that these variants do not modify either the respond to selective TKI (Supplementary Fig. S5). Altogether, our results indicate that tyrosine kinase activity is inhibited in the FGFR4-Ala585Thr and VEGFR3-Leu1014Phe variants, whereas the other variants tested showed unaltered kinase activity. Thus, none of the tested mutations seems to activate the tyrosine kinase domain.

Each mutation was inserted into the 3D representation of the crystal structure of the relevant kinase domain, when available, to visualize its location with respect to the kinase subdomains (Figs. 3B, D, F, H, and J and 4B and D). As the crystal structure of the VEGFR3 kinase domain was unavailable and as the kinase domains of VEGFR1 and VEGFR3 display high homology (see their AA alignment in Supplementary Fig. S6), the VEGFR1 Leu999Phe mutation corresponding to the VEGFR3-Leu1014Phe mutation was inserted into the 3D structure of VEGFR1 (Fig. 4D). The mutations appeared distributed over the various kinase subdomains.

To evaluate the transforming properties of the WT and mutated RTKs, the corresponding expression vectors were used to transfect NIH3T3 fibroblasts, and colony formation was estimated 2 weeks later. As expected, transfection with the HRAS G12V oncogene efficiently induced NIH3T3 transformation (Fig. 5). Pictures of the NIH3T3 plates are shown in Supplementary Fig. S7. Among the WT receptors, only KIT and TRKB induced a statistically significant colony formation increase as compared with the empty vector, and to a lesser extent than HRAS G12V. No mutated receptor was found to increase colony formation significantly. The only variant displaying any effect on NIH3T3 transformation was KIT Pro875Ile. This variant actually had a negative effect, suggesting that the corresponding mutation affects the transforming capacity of the receptor. Because FGFR4 WT and VEGFR3 WT induced no NIH3T3 transformation, it was impossible to evaluate whether the studied inactivating mutations in these receptors might negatively affect their transforming capacity. Thus, evaluation of colony formation did not reveal any transforming properties of the different mutated RTKs.

Discussion

Colorectal cancers harbor many well-known somatic alterations, including mutations in KRAS, PI3K, APC, or p53. Recently, thanks to high-throughput sequencing, RTK alterations have also been characterized, including mutations in the HER2 kinase and translocation of TRKA, found infrequently in colorectal cancer but potentially allowing treatment with TKIs targeting them (20–22). In this study, deep high-throughput sequencing revealed 38 mutations in RTKs, only five of which were already referenced in the COSMIC database. This suggests the existence of various RTK mutations in metastatic colorectal cancer, particularly because they were found in a relatively small cohort of 30 patients. To detect somatic mutations specifically, we chose to sequence genomic DNA from adjacent healthy tissue from all 30 patients to eliminate constitutional mutations from our list. We also sequenced genomic DNA from metastases to obtain information about the persistence of these mutations in metastatic lesions. It is worth noting that about 80% of the KRAS, PI3K, and p53

Published OnlineFirst March 29, 2019; DOI: 10.1158/1535-7163.MCT-18-0582

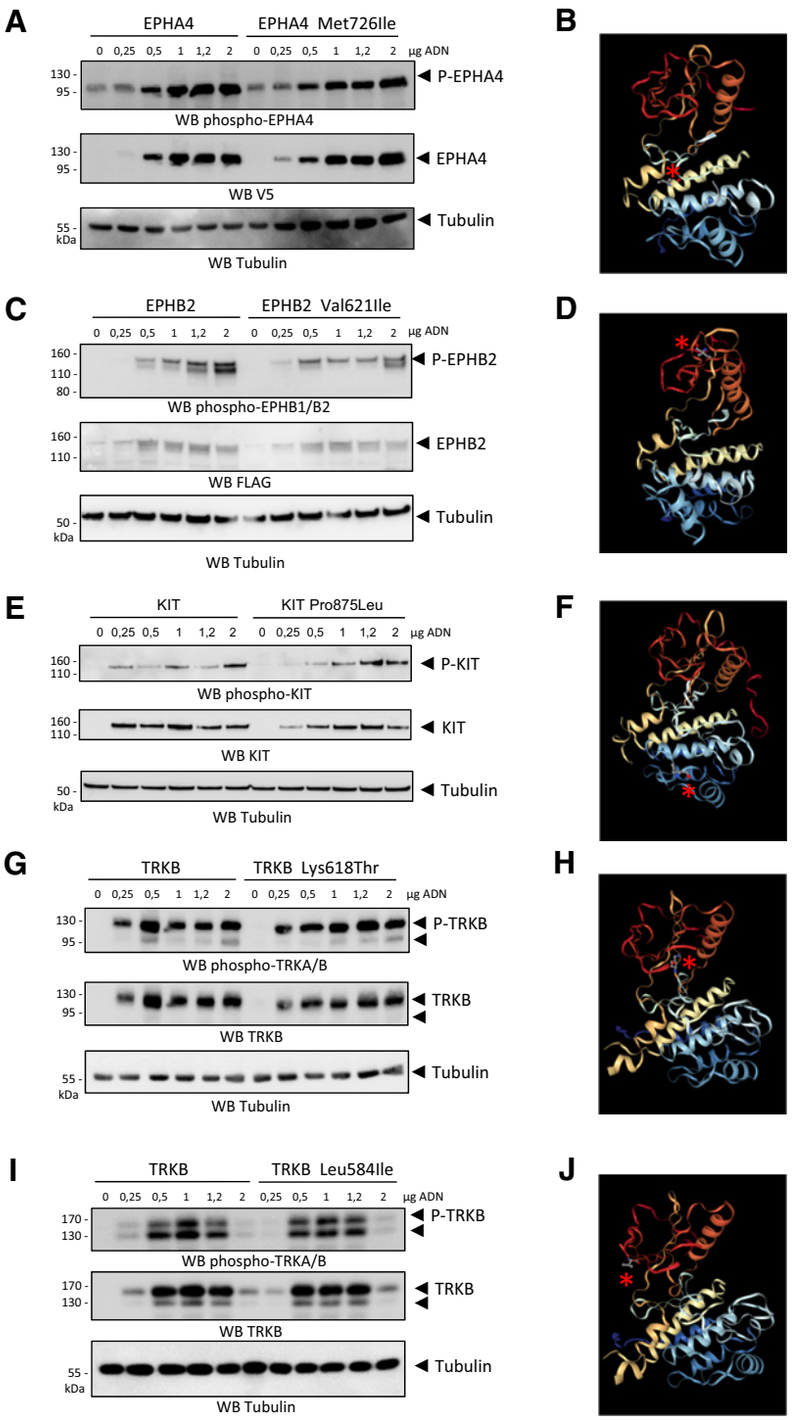

Figure 3.

Tyrosine phosphorylation of EPHA4, EPHB2, KIT, and TRK with somatic mutations in the kinase domain. **A, C, E, G,** and **I,** HEK293T cells were transfected with increasing amounts of a vector expressing the WT or mutated form of the indicated RTK. The empty vector was used at 2-µg transfecting DNA in each case. For each RTK, the same amount of protein was analyzed by Western blotting (WB) with the indicated antibodies directed against either the protein itself or a fused tag (V5 or Flag). Then the blot was reprobed with an antibody directed against the phosphorylated residue(s) of the indicated RTK. Loading was assessed by reprobing with tubulin. Arrowheads indicate the positions of each RTK and of its tyrosine-phosphorylated form. These results are representative of three independent experiments. **B, D, F, H,** and **J,** The mutation of each variant (labeled with an asterisk) was inserted into the 3D structure of its kinase domain.

mutations were found in both the tumor and the metastatic tissue of the patient concerned as expected for driver mutations. The robustness of the sequencing was proved by several independent lines of evidence. Firstly, as all the KRAS, PI3K, and p53 mutations found are described in variant databases, at least for these three genes the sequencing did not yield aberrant variants. Secondly, all the KRAS mutations characterized at diagnosis with SNaPshot were confirmed by targeted NGS. Thirdly, all the RTK mutations selected for further functional analysis were confirmed by Sanger sequencing of genomic DNA from tumors and metastases, whereas they were absent from healthy tissue.

Among the 58 RTKs, less than half harbored somatic mutations and some of them, such as TRKB, VEGFR3, and EPHA5, harbored several different mutations. None of the 38 variants was found in more than one patient, suggesting that each occurs at a low rate. Although 78% of the KRAS, PI3K, and p53 mutations were found

Published OnlineFirst March 29, 2019; DOI: 10.1158/1535-7163.MCT-18-0582

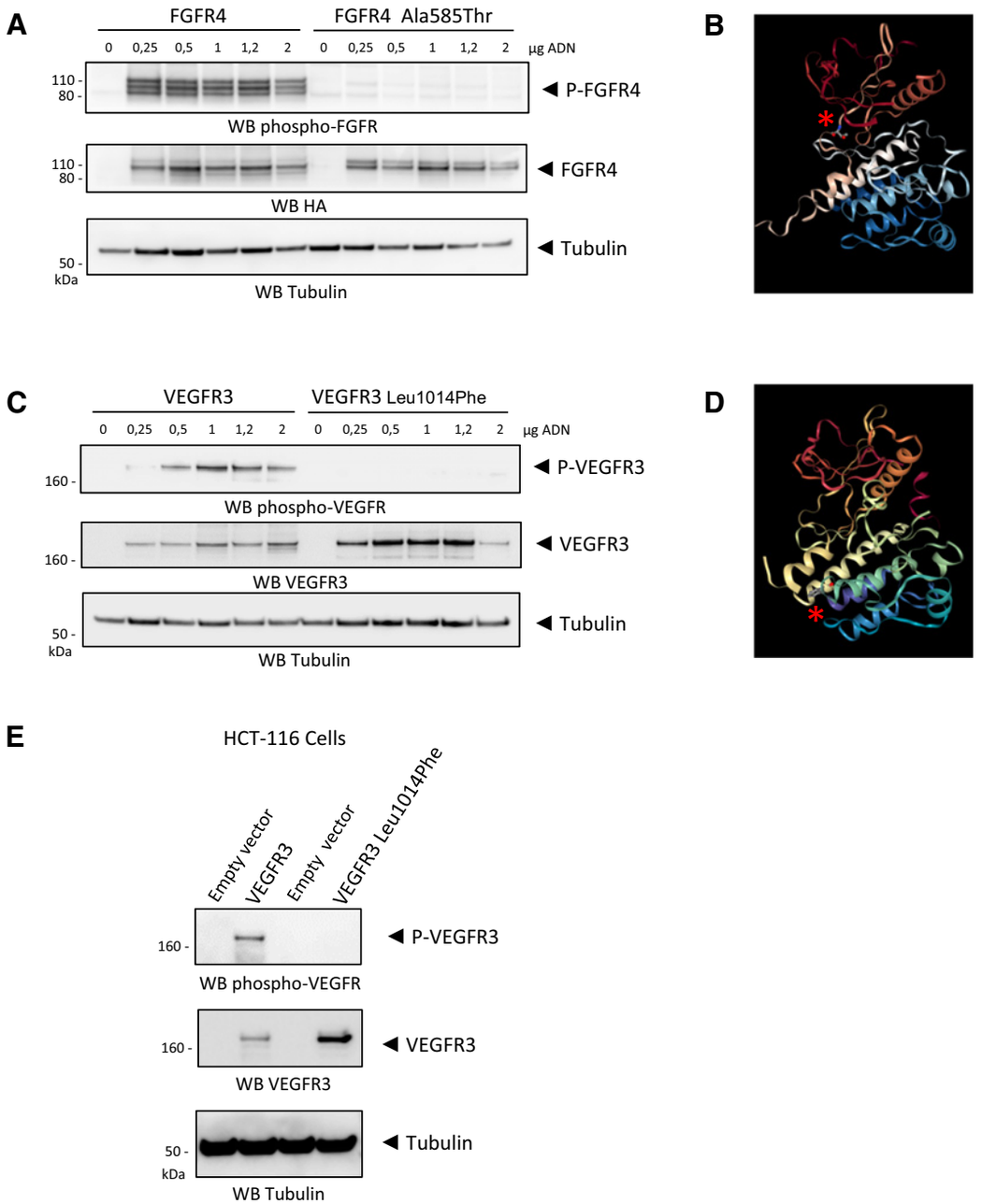

Figure 4.

Tyrosine phosphorylation of FGFR4 and VEGFR3 with somatic mutations in the kinase domain. **A** and **C,** HEK293T cells were transfected with increasing amounts of a vector expressing the WT or mutated form of the indicated RTK. The empty vector was used at 2-µg transfecting DNA in each case. For each RTK, the same amount of protein was analyzed by Western blotting with the indicated antibodies. Then the blot was reprobed with an antibody directed against the phosphorylated residue(s) of the indicated RTK. Loading was assessed by reprobing with tubulin. Arrowheads indicate the positions of each RTK and of its tyrosine-phosphorylated form. These results are representative of three independent experiments. **B** and **D,** The mutation of each variant (labeled with an asterisk) was inserted into the 3D structure of its kinase domain. For VEGFR3 (FLT4), the mutation Leu1014Phe, affecting a residue conserved in VEGFR1, was inserted into the VEGFR1 3D structure. **E,** HCT-116 cells were transfected with 1 µg/mL of empty vector or vector expressing WT or Leu1014Phe VEGFR3. The same amount of protein was analyzed by Western blotting with antibodies directed against VEGFR3. Then, the blot was reprobed with an antibody directed against its tyrosine phosphorylated form. Loading was assessed by reprobing with tubulin. Arrowheads indicate the positions of VEGFR3 and of its tyrosine-phosphorylated form.

in both the tumor tissue and the metastatic tissue from the patient concerned, this was true of only 44% of the mutations affecting RTKs, and the remaining 56% appeared equally distributed between tumors and metastases. Thus, in contrast to the well-known drivers, RTK mutations are not predominantly present in both the tumor and its metastases. As they are not preferentially

Published OnlineFirst March 29, 2019; DOI: 10.1158/1535-7163.MCT-18-0582

present in the metastases either, they do not appear associated with the metastatic process.

In recent years, the number of discovered genomic alterations has increased exponentially, thanks notably to high-throughput sequencing of large tumor cohorts as in The Cancer Genome Atlas project (29). So far, however, only a few activating mutations have been clearly identified. In addition to activating mutations that occur fairly frequently in certain cancer types, such as those altering EGFR in lung cancer (14) or FLT3 in AML (4), recent functional studies have highlighted activating mutations that occur at a relatively low rate, such as the ones affecting ERBB4 in NSCLC (9). A systematic functional analysis of RTK variants in cancer could thus provide important information regarding their involvement or not in the tumorigenic process. Such a functional analysis is possible, thanks to the commercially available antibodies specifically recognizing one or more phosphorylated tyrosine residue(s) in each RTK and to the availability of expression vectors for most RTKs. Here, we show that among seven RTK variants, two displayed a drastic decrease in tyrosine phosphorylation and the other five showed unmodified phosphorylation. NIH3T3 transformation assays confirmed that none of these mutated RTKs had an increased transforming capacity. In contrast to our initial hypothesis that RTK variants located in the kinase domain and present in both tumor and metastasis could be activated mutations, our data suggest that the functionally tested variants do not cause increased kinase activity. Because only activating mutations of RTKs have been shown to be involved in tumorigenesis, the present functional data suggest that the mutations studied are not driver mutations. This precludes the use of TKIs targeting the mutated receptors as a therapeutic strategy.

Analysis of the COSMIC database indicates that several other nonsynonymous variants affecting these RTKs are described in colorectal cancers (with, for instance, 69 variant for EPHA4, 66 for KIT, or 45 for NTRK2). These variants were found all along the coding sequence. Interestingly, to our knowledge, none of these variants was described as activating mutation and it is likely that none functional studies were carried out to investigate their consequence on receptor activation. In light to our current study, demonstrating that none of the testing RTK variants are activating mutations, we can assume that most of the already described rare variants are also nonactivating mutations and are thus unsuitable targets for TKIs. Nevertheless, only extensive functional studies could rule out their adverse impact.

Interestingly, we have found two mutated RTKs (FGFR4-Ala585Thr and FLT4-Leu1014Phe) to display a drastic decrease in tyrosine phosphorylation. One would expect these inactivating mutations to play no role in the transformation process. Yet, a BRAF-inactivating mutation previously reported in patients has recently been shown to play a positive role: the kinase-inactive BRAF Asp631Ala mutant (corresponding to human BRAF Asp594Ala) triggers lung adenocarcinoma in transgenic mice. BRAF inactivation through mutation could thus be an initiating event in lung oncogenesis (30). This counterintuitive effect is explained by enhanced heterodimerization and activation of catalytically competent CRAF in a BRAFAsp631Ala/CRAF complex (31). Interestingly, FGFR4 and VEGFR3 both belong to a subgroup of RTKs showing high homology (FGFR1, 2, 3, and 4 and VEGFR1, 2, and 3). Interestingly, the results of a recent FRET analysis suggest that the presence of FGFR-activating mutations might promote heterodimerization of FGFR (32). Similarly, VEGFR1/VEGFR3 heterodimerization has been evidenced by proximity ligation, and this interaction might be involved in regulating angiogenic sprouting (33). In the light of the regulatory effect of the above-mentioned BRAF-inactivating mutation on the BRAF/CRAF complex, it would be interesting to investigate the influence of FGFR4- and VEGFR3-inactivating mutations on the kinase activity of heterodimers formed with another member of the family.

By adding the identified RTK mutations to the 3D representations of their available crystal structures, we have been able to

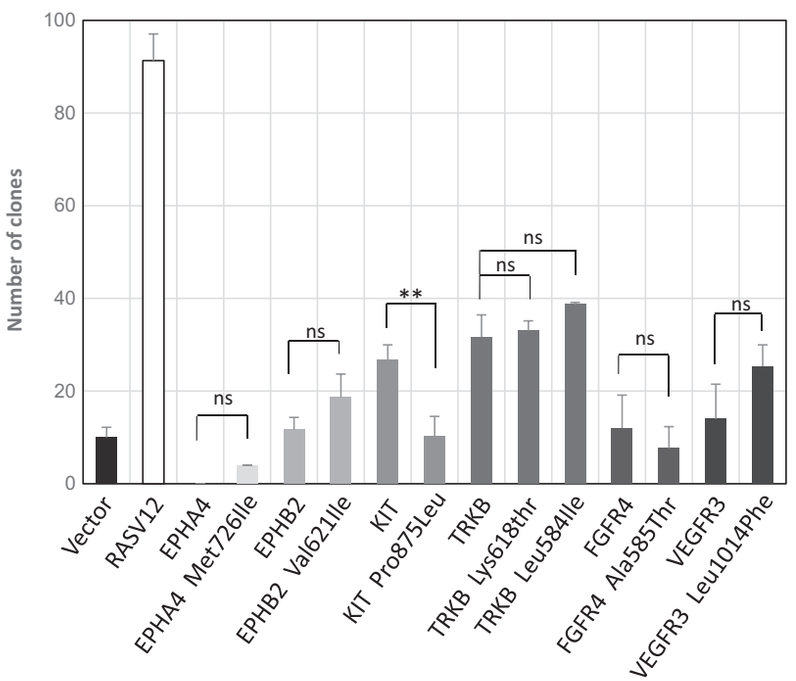

Figure 5.
Fibroblast transformation with the eight RTKs harboring somatic mutations. NIH3T3 cells were transfected with the empty vector or with a vector expressing the indicated WT or mutated RTK or HRAS G12V as a positive control. They were cultured for 15 days in 5% serum and then fixed and stained. Transformed clones were counted. The graph shows the percentage of transformed clones relative to the number obtained with HRAS G12V. **, $P < 0.01$; ns, nonsignificant, as determined by Student's *t* test.

locate them with respect to the kinase subdomains. The FGFR4-inactivating mutation is located near the ATP pocket, which could influence ATP accessibility. The VEGFR3-inactivating mutation lies at the beginning of the second alpha-helix, located C-terminally with respect to the ATP pocket. Interestingly, the mutation in EPHA4 also lies at the beginning of this alpha helix (spatially close to the position of the VEGFR3-inactivating mutation), but we have shown that the EPHA4 mutation does not inactivate the kinase. This highlights the difficulty of predicting the functional consequences of a particular mutation on the sole basis of its location.

To restrict the number of functional analyses, we have focused here on mutations present in the kinase domain and thus likely to be involved in kinase regulation. Yet, mutations localized outside the kinase domain can also influence RTK activity. For instance, it has recently been shown that 3% of NSCLCs display mutations leading to skipping of exon 14 of MET. This in-frame exon skipping causes deletion of the juxtamembrane domain at the N-terminus of the MET kinase domain. The juxtamembrane region is a well-known regulatory domain involved in stabilizing and activating the receptor (34). We, thus, cannot exclude that alterations lying outside the kinase domain might be activating or inhibiting mutations.

The current challenge is no longer to identify somatic mutations, which are increasingly easy to detect, thanks to the development of the high-throughput sequencing. The challenge is rather to interpret these alterations biologically and clinically. Here, we have revealed multiple original RTK mutations in metastatic colorectal cancers, but none of the tested mutations was found to induce activation of the RTK or to increase its transforming capacity. The fact that the mutated RTKs are not activated suggests that they are probably not involved in tumorigenesis and that treatment with TKIs targeting them would be ineffective. Therefore, in parallel to conducting high-throughput sequencing, it appears important to set up reliable functional assays, ideally usable in molecular diagnosis, to interpret identified variants and classify them as pathogenic or neutral. This functional information could notably influence the choice of a suitable targeted therapy.

Disclosure of Potential Conflicts of Interest

N. Rousseau is an engineer at the biobank of Caen. J.-C. Sabourin is a consultant/advisory board member for Boehringer Ingehleim, MSD, BMS, Astra Zeneca, Merck Serono, and Amgen. No potential conflicts of interest were disclosed by the other authors.

Authors' Contributions

Conception and design: L. Duplaquet, M. Figeac, F. Lepretre, G. Goormachtigh, G. Zalcman, Y. de Launoit, V. Fafeur, D. Tulasne
Development of methodology: L. Duplaquet, M. Figeac, F. Lepretre, N. Sarafan-Vasseur, N. Rousseau, D. Tulasne
Acquisition of data (provided animals, acquired and managed patients, provided facilities, etc.): L. Duplaquet, M. Figeac, F. Lepretre, C. Villenet, S. Sebda, N. Sarafan-Vasseur, M. Bénozène, L. Wicquart, N. Rousseau, S. Truant, P. Michel, J.-C. Sabourin, M.-C. Copin, G. Zalcman, V. Fafeur
Analysis and interpretation of data (e.g., statistical analysis, biostatistics, computational analysis): L. Duplaquet, M. Figeac, F. Lepretre, G. Goormachtigh, L. Beaussire, G. Zalcman, D. Tulasne
Writing, review, and/or revision of the manuscript: L. Duplaquet, M. Figeac, F. Lepretre, N. Sarafan-Vasseur, G. Goormachtigh, S. Truant, G. Zalcman, D. Tulasne
Administrative, technical, or material support (i.e., reporting or organizing data, constructing databases): C. Frandemiche, A. Vinchent, G. Goormachtigh, S. Truant, F.B. Galateau-Salle, M.-C. Copin
Study supervision: D. Tulasne

Acknowledgments

This work was supported by the Centre National de la Recherche Scientifique, the Institut Pasteur de Lille (Lille, France), and INSERM, and by grants from the "Cancéropôle Nord-Ouest" (to V. Fafeur and D. Tulasne), the "Ligue Contre le Cancer, Comité Nord" (to D. Tulasne), and the "Institut National du Cancer" (to D. Tulasne). We would like to thank Dr. Liebl, Dr. Elenius, Dr. Klein, Dr. Kaijalainen, Dr. Lu, Dr. Dubreuil, Dr. Alitalo, and Dr. Ittmann for providing the RTK expression vectors. We would like to thank the Centre de Traitement des Données du Cancéropôle Nord-Ouest for clinical data processing.

The costs of publication of this article were defrayed in part by the payment of page charges. This article must therefore be hereby marked *advertisement* in accordance with 18 U.S.C. Section 1734 solely to indicate this fact.

Received May 30, 2018; revised October 8, 2018; accepted March 21, 2019; published first March 29, 2019.

References

1. Lemmon MA, Schlessinger J. Cell signaling by receptor tyrosine kinases. Cell 2010;141:1117–34.
2. Shigematsu H, Gazdar AF. Somatic mutations of epidermal growth factor receptor signaling pathway in lung cancers. Int J Cancer 2006; 118:257–62.
3. Nagata H, Worobec AS, Oh CK, Chowdhury BA, Tannenbaum S, Suzuki Y, et al. Identification of a point mutation in the catalytic domain of the protooncogene c-kit in peripheral blood mononuclear cells of patients who have mastocytosis with an associated hematologic disorder. Proc Natl Acad Sci U S A 1995;92:10560–4.
4. Yamamoto Y, Kiyoi H, Nakano Y, Suzuki R, Kodera Y, Miyawaki S, et al. Activating mutation of D835 within the activation loop of FLT3 in human hematologic malignancies. Blood 2001;97:2434–9.
5. Janoueix-Lerosey I, Lequin D, Brugieres L, Ribeiro A, de Pontual L, Combaret V, et al. Somatic and germline activating mutations of the ALK kinase receptor in neuroblastoma. Nature 2008;455:967–70.
6. Komi DEA, Rambasek T, Wohrl S. Mastocytosis: from a molecular point of view. Clin Rev Aller Immunol 2017;54:397–411.
7. Barlesi F, Mazieres J, Merlio JP, Debieuvre D, Mosser J, Lena H, et al. Routine molecular profiling of patients with advanced non-small-cell lung cancer: results of a 1-year nationwide programme of the French Cooperative Thoracic Intergroup (IFCT). Lancet 2016;387:1415–26.
8. Schmidt L, Duh FM, Chen F, Kishida T, Glenn G, Choyke P, et al. Germline and somatic mutations in the tyrosine kinase domain of the MET proto-oncogene in papillary renal carcinomas. Nat Genet 1997;16: 68–73.
9. Kurppa KJ, Denessiouk K, Johnson MS, Elenius K. Activating ERBB4 mutations in non-small cell lung cancer. Oncogene 2016;35:1283–91.
10. Dimitriou F, Braun RP, Mangana J. Update on adjuvant melanoma therapy. Curr Opin Oncol 2017;30:118–24.
11. Kayser S, Levis MJ. Advances in targeted therapy for acute myeloid leukaemia. Br J Haematol 2017;180:484–500.
12. Oberndorfer F, Mullauer L. Molecular pathology of lung cancer: current status and perspectives. Curr Opin Oncol 2017;30:69–76.
13. Duplaquet L, Kherrouche Z, Baldacci S, Jamme P, Cortot AB, Copin MC, et al. The multiple paths towards MET receptor addiction in cancer. Oncogene 2018;37:3200–15.
14. Paez JG, Janne PA, Lee JC, Tracy S, Greulich H, Gabriel S, et al. EGFR mutations in lung cancer: correlation with clinical response to gefitinib therapy. Science 2004;304:1497–500.

Published OnlineFirst March 29, 2019; DOI: 10.1158/1535-7163.MCT-18-0582

15. Ferlay J, Shin HR, Bray F, Forman D, Mathers C, Parkin DM. Estimates of worldwide burden of cancer in 2008: GLOBOCAN 2008. Int J Cancer 2010; 127:2893–917.
16. Adam R, Hoti E, Folprecht G, Benson AB. Accomplishments in 2008 in the management of curable metastatic colorectal cancer. Gastrointest Cancer Res 2009;3:S15–22.
17. Akkad J, Bochum S, Martens UM. Personalized treatment for colorectal cancer: novel developments and putative therapeutic strategies. Langenbecks Arch Surg 2015;400:129–43.
18. Graham DM, Coyle VM, Kennedy RD, Wilson RH. Molecular subtypes and personalized therapy in metastatic colorectal cancer. Curr Colorect Cancer Rep 2016;12:141–50.
19. Huang D, Sun W, Zhou Y, Li P, Chen F, Chen H, et al. Mutations of key driver genes in colorectal cancer progression and metastasis. Cancer Metastasis Rev 2018;37:173–87.
20. Cancer Genome Atlas Network. Comprehensive molecular characterization of human colon and rectal cancer. Nature 2012;487:330–7.
21. Kavuri SM, Jain N, Galimi F, Cottino F, Leto SM, Migliardi G, et al. HER2 activating mutations are targets for colorectal cancer treatment. Cancer Discov 2015;5:832–41.
22. Ardini E, Bosotti R, Borgia AL, De Ponti C, Somaschini A, Cammarota R, et al. The TPM3-NTRK1 rearrangement is a recurring event in colorectal carcinoma and is associated with tumor sensitivity to TRKA kinase inhibition. Mol Oncol 2014;8:1495–507.
23. Cunningham D, Humblet Y, Siena S, Khayat D, Bleiberg H, Santoro A, et al. Cetuximab monotherapy and cetuximab plus irinotecan in irinotecan-refractory metastatic colorectal cancer. N Engl J Med 2004;351:337–45.
24. Khambata-Ford S, Garrett CR, Meropol NJ, Basik M, Harbison CT, Wu S, et al. Expression of epiregulin and amphiregulin and K-ras mutation status predict disease control in metastatic colorectal cancer patients treated with cetuximab. J Clin Oncol 2007;25:3230–7.
25. Rolfo C, Ruiz R, Giovannetti E, Gil-Bazo I, Russo A, Passiglia F, et al. Entrectinib: a potent new TRK, ROS1, and ALK inhibitor. Expert Opin Investig Drugs 2015;24:1493–500.
26. Paumelle R, Tulasne D, Leroy C, Coll J, Vandenbunder B, Fafeur V. Sequential activation of ERK and repression of JNK by scatter factor/hepatocyte growth factor in madin-darby canine kidney epithelial cells. Mol Biol Cell 2000;11:3751–63.
27. Makarova O, Kamberov E, Margolis B. Generation of deletion and point mutations with one primer in a single cloning step. Biotechniques 2000;29: 970–2.
28. Tulasne D, Paumelle R, Weidner KM, Vandenbunder B, Fafeur V. The multisubstrate docking site of the MET receptor is dispensable for MET-mediated RAS signaling and cell scattering. Mol Biol Cell 1999;10:551–65.
29. Weinstein JN, Collisson EA, Mills GB, Shaw KR, Ozenberger BA, Ellrott K, et al. The Cancer Genome Atlas Pan-Cancer analysis project. Nat Genet 2013;45:1113–20.
30. Nieto P, Ambrogio C, Esteban-Burgos L, Gomez-Lopez G, Blasco MT, Yao Z, et al. A Braf kinase-inactive mutant induces lung adenocarcinoma. Nature 2017;548:239–43.
31. Heidorn SJ, Milagre C, Whittaker S, Nourry A, Niculescu-Duvas I, Dhomen N, et al. Kinase-dead BRAF and oncogenic RAS cooperate to drive tumor progression through CRAF. Cell 2010;140:209–21.
32. Del Piccolo N, Sarabipour S, Hristova K. A new method to study heterodimerization of membrane proteins and its application to fibroblast growth factor receptors. J Biol Chem 2017;292:1288–301.
33. Nilsson I, Bahram F, Li X, Gualandi L, Koch S, Jarvius M, et al. VEGF receptor 2/-3 heterodimers detected in situ by proximity ligation on angiogenic sprouts. EMBO J 2010;29:1377–88.
34. Cortot AB, Kherrouche Z, Descarpentries C, Wislez M, Baldacci S, Furlan A, et al. Exon 14 deleted MET receptor as a new biomarker and target in cancers. J Natl Cancer Inst 2017;109.

Published OnlineFirst March 29, 2019; DOI: 10.1158/1535-7163.MCT-18-0582

Molecular Cancer Therapeutics

Functional Analysis of Somatic Mutations Affecting Receptor Tyrosine Kinase Family in Metastatic Colorectal Cancer

Leslie Duplaquet, Martin Figeac, Frédéric Leprêtre, et al.

Mol Cancer Ther 2019;18:1137-1148. Published OnlineFirst March 29, 2019.